Anal. Chem. **2008,** *80,* 1058−1066

Magic Angle Spinning NMR and $^{1}H-^{31}P$ Heteronuclear Statistical Total Correlation Spectroscopy of Intact Human Gut Biopsies

Yulan Wang,*,† Olivier Cloarec,† Huiru Tang,‡ John C. Lindon,† Elaine Holmes,† Sunil Kochhar,§ and Jeremy K. Nicholson*,†

Department of Biomolecular Medicine, SORA Division, Faculty of Medicine, Imperial College London, Sir Alexander Fleming Building, South Kensington, London SW7 2AZ UK, State Key Laboratory of Magnetic Resonance and Atomic and Molecular Physics, Wuhan Centre for Magnetic Resonance, Wuhan Institute of Physics and Mathematics, The Chinese Academy of Sciences, Wuhan, 430071, PR China, and Nestlé Research Center, Lausanne, Nestec Ltd., Vers-Chez-Les-Blanc, 1000 Lausanne 26, Switzerland

Previously we have demonstrated the use of ^{1}H magic angle spinning (MAS) NMR spectroscopy for the topographical variations in functional metabolic signatures of intact human intestinal biopsy samples. Here we have analyzed a series of MAS ^{1}H NMR spectra (spin−echo, one-dimensional, and diffusion-edited) and $^{31}P-\{^{1}H\}$ spectra and focused on analyzing the enhancement of information recovery by use of the statistical total correlation spectroscopy (STOCSY) method. We have applied a heterospectroscopic cross-examination performed on the same samples and between ^{1}H and $^{31}P-\{^{1}H\}$ spectra (heteronuclear STOCSY) to recover latent metabolic information. We show that heterospectroscopic correlation can give new information on the molecular compartmentation of metabolites in intact tissues, including the statistical "isolation" of a phosphlipid/triglyceride vesicle pool in intact tissue. The application of $^{31}P-^{1}H$ HET-STOCSY allowed the cross-assignment of major ^{31}P signals to their equivalent ^{1}H NMR spectra, e.g., for phosphorylcholine and phosphorylethanolamine. We also show pathway correlations, e.g., the ascorbate−glutathione pathway, in the STOCSY analysis of intact tissue spectra. These $^{31}P-^{1}H$ HET-STOCSY spectra also showed different topographical regions, particular for minor signals in different tissue microenvironments. This approach could be extended to allow the detection of altered distributions within metabolic subcompartments as well as conventional metabonomics concentration-based diagnostics.

The successful application of metabonomics and related approaches[1−3] to disease classification relies on the quantitative or semiquantitative description of the metabolic signature of cells, tissues, or biofluids derived from analytical technologies such as nuclear magnetic resonance (NMR) spectroscopy[4] and mass spectrometry (MS) coupled to gas chromatographic[5] or liquid chromatographic separation methods.[6] NMR spectroscopy has been widely and successfully used to measure multiple endogenous metabolites simultaneously in a variety of tissues and biofluids in a range of physiological and pathological states.[1,7−14] When combined with multivariate statistical techniques, such studies have efficiently enabled the discovery of novel biomarker combinations.[15] A unique feature of NMR spectroscopy as a structural analytical tool is its nondestructive nature that allows biofluids,[13,16] cells,[17] and intact tissues, and even the dynamic biochemical reactions in those systems, to be measured and monitored through time noninvasively.[18]

* To whom correspondence should be addressed. Tel: 44(0) 20 7594 3195. Fax: 44(0) 20 7594 3226. E-mail: yulan.wang@imperial.ac.uk; j.nicholson@imperial.ac.uk.

† Imperial College London.

‡ Wuhan Institute of Physics and Mathematics.

§ Nestec Ltd.

(1) Nicholson, J. K.; Lindon, J. C.; Holmes, E. *Xenobiotica* **1999**, *29*, 1181−1189.

(2) Tweeddale, H.; Notley-McRobb, L.; Ferenci, T. *J. Bacteriol.* **1998**, *180*, 5109−5116.

(3) Tang, H. R.; Wang, Y. L. *Prog. Biochem. Biophys.* **2006**, *33*, 401−417.

(4) Claridge, T. D. W. *High-Resolution NMR Techniques in Orgnaic Chemistry*; Oxford University Press: Oxford, UK, 1999.

(5) Fancy, S. A.; Beckonert, O.; Darbon, G.; Yabsley, W.; Walley, R.; Baker, D.; Perkins, G. L.; Pullen, F. S.; Rumpel, K. *Rapid Commun. Mass Spectrom.* **2006**, *20*, 2271−2280.

(6) Wilson, I. D.; Plumb, R.; Granger, J.; Major, H.; Williams, R.; Lenz, E. A. *J. Chromatogr., B: Anal. Technol. Biomed. Life Sci.* **2005**, *817*, 67−76.

(7) Lindon, J. C.; Nicholson, J. K.; Holmes, E.; Everett, J. R. *Concepts Magn. Reson.* **2000**, *12*, 289−320.

(8) Nicholson, J. K.; Connelly, J.; Lindon, J. C.; Holmes, E. *Nat. Rev. Drug Discovery* **2002**, *1*, 153−161.

(9) Nicholson, J. K.; Wilson, I. D. *Nat Rev Drug Discov* **2003**, *2*, 668−676.

(10) Waterfield, C. J.; Turton, J. A.; Scales, M. D. C.; Timbrell, J. A. *Toxicology* **1993**, *77*, 1−5.

(11) Wang, Y. L.; Bollard, M. E.; Nicholson, J. K.; Holmes, E. *J. Pharm. Biomed. Anal.* **2006**, *40*, 375−381.

(12) Nicholls, A. W.; Mortishire-Smith, R. J.; Nicholson, J. K. *Chem. Res. Toxicol.* **2003**, *16*, 1395−1404.

(13) Wang, Y. L.; Holmes, E.; Nicholson, J. K.; Cloarec, O.; Chollet, J.; Tanner, M.; Singer, B. H.; Utzinger, J. *Proc. Natl. Acad. Sci. U.S.A.* **2004**, *101*, 12676−12681.

(14) Wang, Y. L.; Utzinger, J.; Xiao, S. H.; Xue, J.; Nicholson, J. K.; Tanner, M.; Singer, B. H.; Holmes, E. *Mol. Biochem. Parasitol.* **2006**, *146*, 1−9.

(15) Holmes, E.; Nicholson, J. K.; Nicholls, A. W.; Lindon, J. C.; Connor, S. C.; Polley, S.; Connelly, J. *Chemom. Intell. Lab. Syst.* **1998**, *44*, 245−255.

(16) Wang, Y. L.; Holmes, E.; Tang, H. R.; Lindon, J. C.; Sprenger, N.; Turini, M. E.; Bergonzelli, G.; Fay, L. B.; Kochhar, S.; Nicholson, J. K. *J. Proteome Res.* **2006**, *5*, 1535−1542.

(17) Anthony, M. L.; McDowell, P. C. R.; Gray, T. J. B.; Blackmore, M.; Nicholson, J. K. *Biomarkers* **1996**, *1*, 35−43.

10.1021/ac701988a CCC: $40.75
Published on Web 01/19/2008

In vivo magnetic resonance spectroscopy (MRS) has been widely applied to study metabolism, but it has low spatial resolution (0.5−1 mm^3) and sensitivity and limited range of metabolites present in high cellular concentrations such as choline, glutamate, *N*-acetylaspartate, creatine, lactate, and lipids in a variety of tissues.[19]

Disease-induced cellular damage is associated with characteristic disruptions of cellular metabolic processes and changes in patterns of metabolite concentrations.[9,20] While studies using biofluids provide a whole systems evaluation of metabolic effects, investigation of individual tissues allows much more localized effects to be uncovered.

For tissue biopsies and other ex vivo samples, high-resolution magic angle spinning (HRMAS) ^{1}H NMR spectroscopy has been shown to be highly effective in revealing a much wider range of cellular metabolites than is possible with in vivo MRS and for obtaining novel metabolic descriptors for disease in man and in animals. This is especially true when combined with pattern recognition methods.[11,21,22] The MAS process removes the residual anisotropic spin interactions such as dipolar couplings, chemical shift anisotropy contributions in the spectra, and certain effects of magnetic field inhomogeneities resulting in a spectral resolution comparable to liquid-state NMR spectroscopy.[22,23]

Important metabolic parameters that have hardly been exploited are molecular dynamics effects such as restricted diffusion and cellular compartmentation effects, these being accessed via NMR measured diffusion coefficients and relaxation times.[24] Although little is known about variations in compartmentation and molecular mobility of metabolites between tissue types and in disease states because of the difficulties involved in capturing multivariate metabolic information at high spectral or spatial resolution, some previous studies have showed that NMR spectroscopy is useful in capturing compartmental information.[25]

Another significant methodological development for the recovery of metabolic biomarker information from NMR and MS data, either alone or in combination, has centered on the new concept of "statistical spectroscopy", which has been exemplified in two forms, *s*tatistical *to*tal *c*orrelation *s*pectroscop*y* (STOCSY)[26] and *s*tatistical *h*eterospectroscop*y*[27] for biofluid analysis. The power of STOCSY relies on the linear covariation between NMR signal intensities from nuclei in the same molecules when measured under identical conditions across many samples containing different levels of the compounds.[26] The approach is an extension of generalized two-dimensional correlation spectroscopy as proposed and developed by Noda[28] and recently reviewed by Huang[29] and has previously been applied to analyze NMR data from single samples using the correlation approach as an alternative to the second FT in 2D NMR studies.[30] The analysis is based on calculation of the correlation matrices for every data point in the spectra of all samples of interest. The correlation coefficients are subsequently replotted in a two-dimensional δ versus δ matrix, which appears analogous to the conventional two-dimensional total correlation spectroscopy NMR experiment that can be applied to single samples. Recently, heteronuclear STOCSY (HET-STOCSY), i.e., correlating ^{1}H and ^{31}P NMR spectra, has been applied to intact liver tissue in order to aid the identification of phosphorus-containing compounds.[31] The key advantages of STOCSY include increased sensitivity (because many samples are analyzed together, improving signal-to-noise ratios) and the nonreliance of the atomic or molecular connectivity on any of the NMR-based parameters such as J couplings or nuclear Overhauser effect (NOE) that are required for all conventional two-dimensional NMR spectroscopic measurements.

Previously, we analyzed human gut biopsy tissues individually using ^{1}H NMR spectroscopy[32] in order to derive metabolic differences between the tissues taken from different parts of the gut and their relationships with differential physiological functions, and this has been reported in a separate publication.[32] Here, we describe the application of a novel extension of the STOCSY approach to statistically integrate heterospectroscopic data sets derived from multiple homonuclear and heteronuclear ^{1}H MAS NMR spectra (standard, spin−echo, and diffusion-edited) and standard MAS proton-decoupled ^{31}P (denoted as ^{31}P−{^{1}H}) spectra (Figure 1) collected sequentially on multiple gut epithelial biopsy samples (n = 75) obtained from human participants at five different levels of the gut (antrum, duodenum, jejunum, ileum, and transverse colon). The main aim of these studies was to investigate the use of STOCSY-based methods to recover metabolic subcompartmentational data by coanalysis of spectra that contain latent motional and dynamic information.

MATERIALS AND METHODS

Sample Collection. The study protocol was approved by the Etat de Vaud, Lausanne, Switzerland. Human biopsies from the gut intestinal tract, namely, antrum, duodenum, jejunum, ileum, and transverse colon, were obtained from 8 male and 8 female healthy participants by endoscopy or colonoscopy under sedation (Dormicum 2.5−5 mg IV and/or Pethidine 25−50 mg IV). The participants had not been taking any drugs or anticoagulation treatment during the 4 weeks before sampling. The participants were required to fast for 12 h and took a routinely used bowel preparation on the evening before the procedure. Biopsies were

(18) Holmes, E.; Bonner, F. W.; Sweatman, B. C.; Lindon, J. C.; Beddell, C. R.; Rahr, E.; Nicholson, J. K. *Mol. Pharmacol.* **1992**, *42*, 922−930.
(19) Choi, I. Y.; Lee, S. P.; Merkle, H.; Shen, J. *Neuroimage* **2006**, *33*, 85−93.
(20) Nicholson, J. K.; Wilson, I. D. *Prog Nucl Magn. Reson. Spectrosc.* **1989**, *21*, 449−501.
(21) Wold, S.; Esbensen, K.; Geladi, P. *Chemom. Intell. Lab. Syst.* **1987**, *2*, 37−52.
(22) Wang, Y. L.; Tang, H. R.; Holmes, E.; Lindon, J. C.; Turini, M. E.; Sprenger, N.; Bergonzelli, G.; Fay, L. B.; Kochhar, S.; Nicholson, J. K. *J. Proteome Res.* **2005**, *4*, 1324−1329.
(23) Bollard, M. E.; Garrod, S.; Holmes, E.; Lincoln, J. C.; Humpfer, E.; Spraul, M.; Nicholson, J. K. *Magn. Reson. Med.* **2000**, *44*, 201−207.
(24) Belton, P. S.; Ratcliffe, R. G. *Prog. Nucl. Magn. Reson. Spectrosc.* **1985**, *17*, 241−279.
(25) Larkin, T. J.; Bubb, W. A.; Kuchel, P. W. *Biophys. J.* **2007**, *92*, 1770−1776.
(26) Cloarec, O.; Dumas, M. E.; Craig, A.; Barton, R. H.; Trygg, J.; Hudson, J.; Blancher, C.; Gauguier, D.; Lindon, J. C.; Holmes, E.; Nicholson, *J. Anal. Chem.* **2005**, *77*, 1282−1289.
(27) Crockford, D. J.; Holmes, E.; Lindon, J. C.; Plumb, R. S.; Zirah, S.; Bruce, S. J.; Rainville, P.; Stumpf, C. L.; Nicholson, J. K. *Anal. Chem.* **2006**, *78*, 363−371.
(28) Noda, I.; Dowrey, A. E.; Marcott, C.; Story, G. M.; Ozaki, Y. *Appl. Spectrosc.* **2000**, *54*, 236A−248A.
(29) Huang, H. *Anal. Chem.* **2007**, *79*, 8281−8292.
(30) Chen, Y. B.; Zhang, F. L.; Bermel, W.; Bruschweiler, R. *J. Am. Chem. Soc.* **2006**, *128*, 15564−15565.
(31) Coen, M.; Hong, Y. S.; Cloarec, O.; Rhode, C.; Reily, M. D.; Robertson, D.; Holmes, E.; Lindon, J. C.; Nicholson, J. K. *Anal. Chem.* **2007**, *79*, 8956−8966.
(32) Wang, Y. L.; Holmes, E.; Comelli, E. M.; Fotopoulos, G.; Dorta, G.; Tang, H. R.; Rantalainen, M.; Lindon, J. C.; Corthesy-Theulaz, I.; Fay, L. B.; Kochhar, S.; Nicholson, J. K. *J. Proteome Res.* **2007**, *6*, 3944−3951.

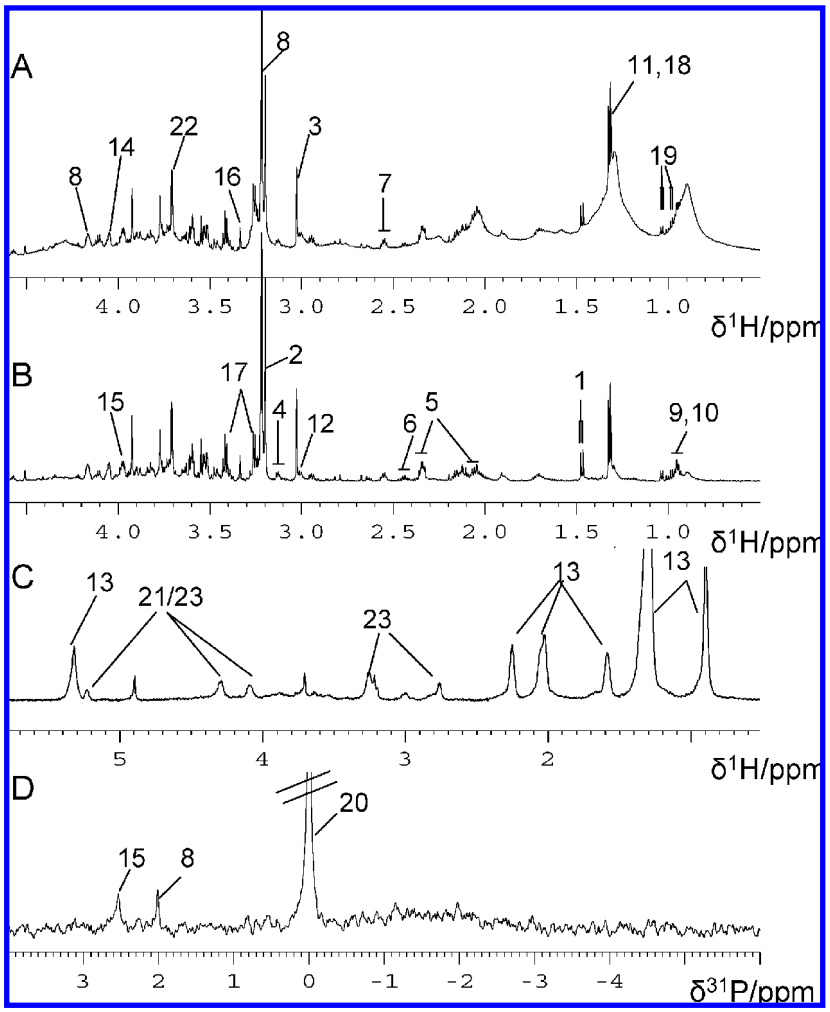

Figure 1. HRMAS NMR spectra of a human ileum biopsy sample. (A) One-dimensional ^{1}H NMR; (B) CPMG spin−echo ^{1}H NMR; (C) diffusion-edited ^{1}H NMR; and (D) proton-decoupled ^{31}P−{^{1}H} NMR spectrum. Key: 1, alanine; 2, choline; 3, creatine; 4, ethanolamine; 5, glutamate; 6, glutamine; 7, glutathione; 8, phosphorylcholine; 9, isoleucine; 10, leucine; 11, lactate; 12, lysine; 13, fatty acyl group peaks from lipids; mostly triglycerides; 14, *myo*-inositol; 15, phosphorylethanolamine; 16, *scyllo*-inositol; 17, taurine; 18, threonine; 19, valine; 20, inorganic phosphate; 21, glyceryl peaks from triglycerides and phospholipids; 22, contamination from bowel preparation; 23, choline moiety of phospholipids.

snap-frozen immediately after collection and stored at −80 °C until NMR spectroscopic analysis. Details of the standard spectroscopic profiles of these samples have recently been published showing anatomical region-specific differences in metabolic profiles.[32]

High-Resolution MAS NMR Spectroscopy. Samples of biopsy tissue, each ∼15 mg, were soaked with deuterated water and packed into separate 4-mm-diameter zirconium oxide rotors with spherical inserts and Kel-F caps. NMR experiments were performed on a Bruker DRX-600 spectrometer equipped with a triple resonance (^{1}H/^{13}C/^{31}P) high-resolution MAS probe with pulsed-field gradient capability along the magic angle axis (Bruker Biospin, Rheinstetten, Germany), operating at a 600.13 MHz for ^{1}H, and 243.93 MHz for ^{31}P observation. Samples were spun at 5 kHz at the magic angle and maintained at a constant temperature of 283 K. Three different types of one-dimensional ^{1}H NMR spectra and a one-dimensional proton decoupled ^{31}P spectrum (denoted ^{31}P−{^{1}H} were acquired sequentially for each sample. The 90° pulse lengths were typically 9.0−10 μs for ^{1}H and 8 μs for ^{31}P. The data collection was achieved in the following sequence for each sample: (a) a standard one-dimensional ^{1}H spectrum with water suppression using the pulse sequence −RD−90°−t_1−90°−t_m−90°−ACQ−,[33] where the interpulse delay t_1 was 3 μs, the mixing time t_m was 150 ms and with a weak irradiation applied at the water resonance during both the mixing time and the recycle delay, (RD), with ACQ representing the data acquisition time, (b) a water-suppressed Carr−Purcell−Meiboom−Gill (CPMG) spin−echo spectrum using the pulse sequence −RD-90°−$(\tau-180°-\tau)_n$−ACQ−,[34] with a total spin−spin relaxation delay (2nτ) of 200 ms and water signal irradiation being applied during the recycle delay, (c) a water-suppressed diffusion-edited ^{1}H NMR spectrum to remove peaks from low molecular weight components using the bipolar-pair longitudinal eddy current (BPP-LED) pulse sequence, −RD−90°−G_1−τ−180°−G_2−τ−90°−Δ−90°−G_3−τ−180°−G_4−τ−90°−T_e−90°−ACQ−[35] with a sine-shaped pulsed-field gradient, G, along the magic angle, of strength 32 G/cm and duration of 2.5 ms, a delay (τ) of 400 μs to allow for the decay of eddy currents, a diffusion time (Δ) of 100 ms, and a delay T_e of 5 ms,

(33) Nicholson, J. K.; Foxall, P. J. D.; Spraul, M.; Farrant, R. D.; Lindon, J. C. *Anal. Chem.* **1995**, *67*, 793−811.
(34) Meiboom, S.; Gill, D. *Rev. Sci. Instrum.* **1958**, *29*, 688−691.
(35) Wu, D. H.; Chen, A. D.; Johnson, C. S. *J. Magn. Reson. A* **1995**, *115*, 260−264.

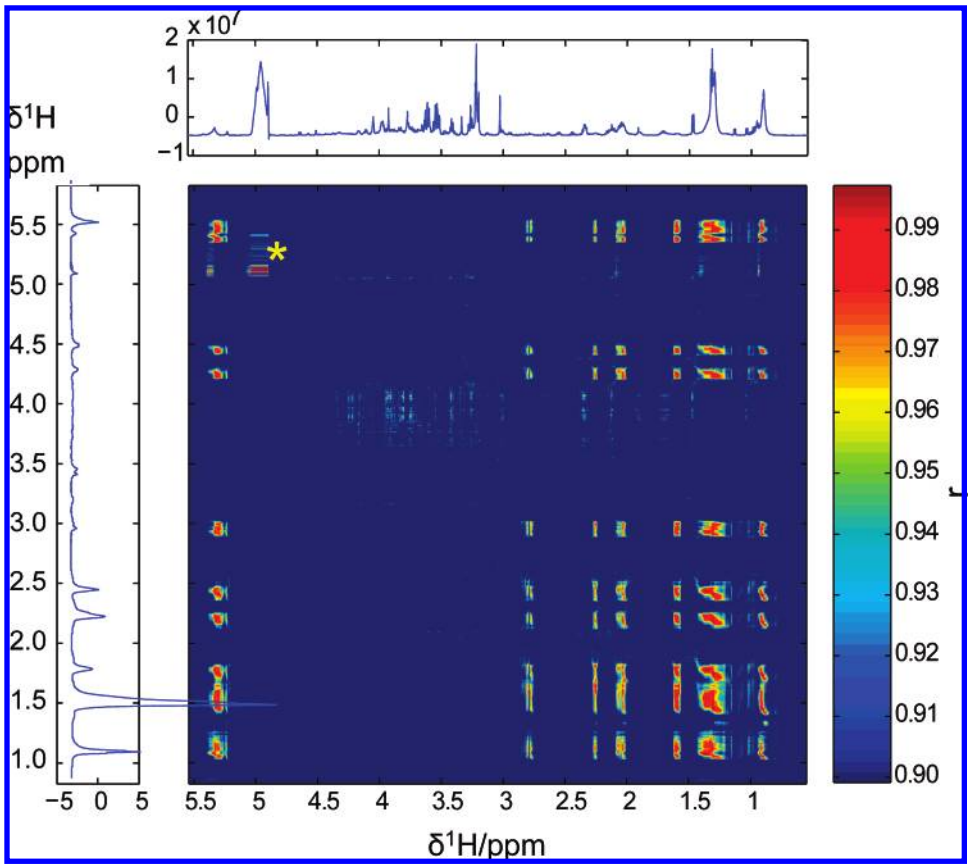

Figure 2. Two-dimensional heterospectroscopic/homonuclear STOCSY correlation map generated from ^{1}H diffusion-edited and CPMG spin−echo MAS NMR spectra obtained from transverse colon samples; the cross-peaks indicating lipid resonances from triglyceride droplets. * water peak.

with water peak suppression being applied during the recycle delay. For each ^{1}H spectrum, a total of 128 transients were collected into 32k data points with a spectral width of 12 019.23 Hz and a recycle delay, RD, of 2.0 s. Next, a ^{31}P−{^{1}H} MAS NMR spectrum was acquired using a single 90° pulse excitation sequence with broadband proton decoupling. A total of 1024 scans were collected into 16k data points with spectral width of 30 ppm (7309.94 Hz) and a recycle delay of 2.0 s. All the ^{1}H MAS NMR spectra were multiplied by an exponential function equivalent to a 0.3 Hz line-broadening factor, and the ^{31}P−{^{1}H} NMR spectra had 5 Hz line-broadening prior to Fourier transformation. The spectra were corrected for phase and baseline distortions manually using XWINNMR3.5 (Bruker Biospin). The chemical shifts for ^{1}H were calibrated using the center of the alanine doublet resonance taken to be at δ_H1.47, and for the ^{31}P chemical shifts, the inorganic phosphate resonance at δ_P0.00 was used. However, for ^{31}P−^{1}H STOCSY analysis, the ^{31}P NMR chemical shifts were aligned to give the phosphorylcholine resonance at δ_P2.01.

Multivariate Modeling. The spectra over the range δ_H −1 to 10.0 for ^{1}H and the range δ_P −6.0 to 4.0 for ^{31}P were digitized into 22K data points using a MATLAB script developed in-house. STOCSY analysis was subsequently performed on these data sets as described previously.[26]

RESULTS AND DISCUSSION

NMR Spectroscopic Data Sets. Typical MAS NMR spectra of a gut biopsy sample from the ileum are shown in Figure 1. Each spectrum provides different types of metabolic information as well as information on molecular mobility (the CPMG spectra) and translational diffusion of small molecules. The standard 1D spectrum (Figure 1A) shows an envelope of broad signals with superimposed well-resolved peaks, the former arising from macromolecules and substances with constrained molecular motions and the latter from small molecules with short rotational correlation times, while the CPMG spectrum (Figure 1B) is dominated by peaks from signals from low molecular weight compounds, the peaks from macromolecules being attenuated. Conversely, the diffusion-edited spectrum (Figure 1C) using a field gradient strength of 32 G/cm only shows peaks from macromolecules and other highly motionally constrained species that have limited translational diffusion coefficients. Finally, the ^{31}P−{^{1}H} NMR spectrum shows singlet peaks from the major phosphorus-containing metabolites in the tissues (Figure 1D). The ^{1}H NMR spectral assignments were made according to a previous publication[32] and are listed in the caption of Figure 1.

Carrying out the simple ^{1}H−^{1}H STOCSY procedure on a series of spectra from one type of experiment will allow identification of the multiple self-correlation peaks from a given set of molecules. If the intensities are anticorrelated or with a lower correlation coefficient, then the molecules may also be from the same metabolic pathway or in differentially regulated pathways, for example, where one metabolite (A) is an enzyme substrate and the other is its product (B), any variation in enzymatic reaction in a series will lead to varying A/B ratios and hence generate

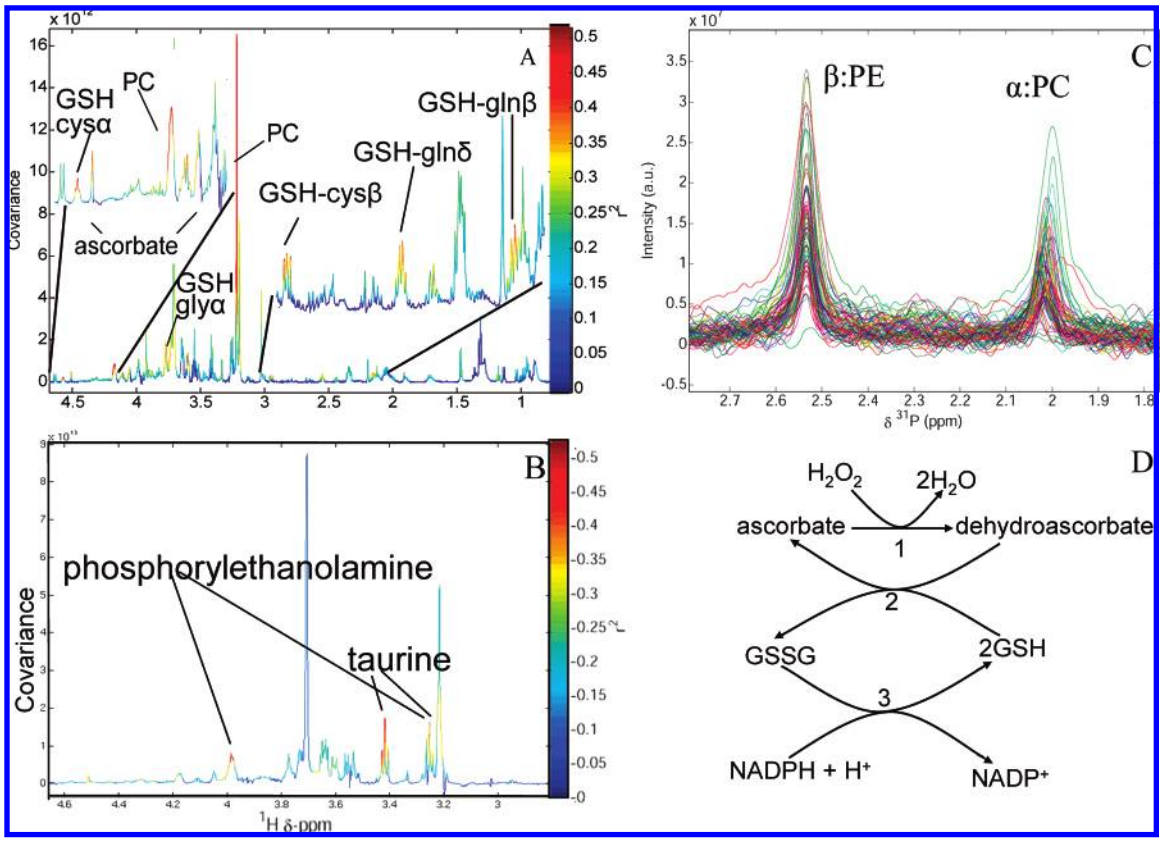

Figure 3. One-dimensional HET-STOCSY plot generated from ^{31}P−{^{1}H} and ^{1}H CPMG NMR spectra from all the samples showing (A) the correlation of the ^{31}P NMR resonance of PC with ascorbate and glutathione and (B) that of PE correlating with taurine and phosphorylethanolamine. (C) An expansion of the ^{31}P−{^{1}H} MAS NMR spectra, showing PC and PE. (D) A schematic diagram of the antioxidant process *via* the ascorbate−glutathione pathway. Step 1 is catalyzed by ascorbate peroxidase, step 2 is catalyzed by dehydroascorbate reductase, and step 3 is catalyzed by glutathione reductase.

anticorrelations. This approach has been exploited previously using biofluids for identification of endogenous metabolites,[26] for example, glycerate, isovalerate, and glutarate. Urinary drug metabolites, such as those of acetaminophen and ibuprofen, have also been identified from population studies using STOCSY.[36] Recently, HET-STOCSY has been successfully applied to ^{31}P and ^{1}H MAS spectra of intact liver tissues to aid the identification of low concentrations of phosphorus containing compounds, such as UDP-*N*-acetylglucosamine and UDP-*N*-acetylgalactosamine.[31]

Cross-Correlation of Different ^{1}H NMR Spectral Data Sets from the Same Sample. The ^{1}H−^{1}H STOCSY approach has been used to carry out cross-correlations between different types of ^{1}H NMR experiments collected from the same samples. Here we have four types of NMR spectra on multiple examples of the same tissue type; these experiments, although homonuclear, are still heterospectroscopic because the different experiments yield different information from the same samples. Such a pairwise statistical correlation gives rise to a series of two-dimensional contour maps, with cross-peaks selected and color-coded to indicate the strong correlations. The types of correlation between different experiments within the same type of samples can be either homonuclear, e.g., ^{1}H−^{1}H, or heteronuclear such as ^{1}H−^{31}P−{^{1}H}. This can be generalized to any pair or multiples of nuclei where there is parallel spectroscopic information.[31] Also, in principle, the statistical coanalysis of true two-dimensional NMR spectra is possible (e.g., ^{1}H−^{1}H TOCSY with ^{31}P−{^{1}H}, or even ^{1}H−^{1}H TOCSY with ^{1}H−^{1}H TOCSY), but this is spectroscopically time demanding as well as computationally demanding. Here to exemplify the approach, we have confined the analysis to 1D datasets only.

Examining the cross-correlation structure for the same type of NMR experiment, e.g., CPMG with CPMG, ^{1}H−STOCSY, it is possible to ascertain the molecular connectivities as described originally for standard 1D NMR experiment STOCSY[26] in order to aid metabolite identification. However, examination of the correlation of different types of NMR spectra, for example, CPMG spin−echo ^{1}H NMR spectra with diffusion-edited ^{1}H NMR spectra obtained from transverse colon biopsies as shown in Figure 2, leads to a different type of information recovery where cross-peaks came from only molecules with slow transverse diffusion as well as having rapid molecular tumbling. Figure 2 shows such a ^{1}H−^{1}H CPMG/diffusion-edited STOCSY cross-correlation plot with the mean diffusion-edited spectrum on the vertical axis and the mean CPMG spectrum on the horizontal axis together with the 2D covariance matrix. The 2D STOCSY matrix contains signals from triglycerides present in lipid droplets, which have very slow diffusion rates because they have large Stoke's radii, but the triglyceride molecules themselves have relatively long T_2 values because they have a high degree of rotational freedom of the fatty acyl chains within the large droplets. We also observed signals

(36) Holmes, E.; Loo, R. L.; Cloarec, O.; Coen, M.; Tang, H. R.; Maibaum, E.; Bruce, S.; Chan, Q.; Elliott, P.; Stamler, J.; Wilson, I. D.; Lindon, J. C.; Nicholson, J. K. *Anal. Chem.* **2007**, *79*, 2629−2640.

from the glyceryl moiety (δ4.3−4.5) in the diffusion-edited spectra because they are from slow-diffusing species, but these signals do not appear in the CPMG spectra or, hence the 2D STOCSY plot, because their T_2 values are short indicating a higher a degree of rigidity of the glyceryl backbone than the flexible fatty acyl groups. From an approximate integration of the NMR peaks from the N^+Me_3 group of phosphotidylcholine (PC) and the CH_2 resonance from the glyceryl moiety of both triglycerides and phospholipids, it is estimated that the lipid droplets comprise ~64% triglyceride and ~36% phospholipids, implying the presence of phospholipid vesicles with triglycerides incorporated inside. We also note that a water peak, marked with an asterisk in Figure 2, also appears in the correlation plot. This is likely to be due to some form of compartmentalized water since free water, with its fast diffusion, is not likely to appear in the diffusion-edited spectrum.

Cross-Correlation of $^{31}P-\{^1H\}$ and ^1H NMR Spectra for ^{31}P NMR Resonance Assignment. The use of the STOCSY approach to evaluate signal intensity covariation in spectra from different nuclei (in this case $^{31}P-\{^1H\}$ and ^1H) in order to make connections between the ^{31}P and ^1H NMR signals is also possible. This allows a linkage between structurally or functionally connected protons on the same or related molecules to the phosphorus atoms. This is a heteronuclear spectroscopic type of STOCSY termed HET-STOCSY,[31] and this has been applied previously to rat liver tissue spectra for assignment of UDP-sugar conjugate peaks.[31] Here we have applied the technique for the first time to human tissue biopsy MAS NMR spectra.

The first task of understanding HET-STOCSY data is to identify the statistical correlations between the phosphorus signal and these in the ^1H NMR spectra (Figure 1D). The $^{31}P-^1H$ HET-STOCSY plot given in Figure 3 shows that peak α (δ_P 2.05) in the $^{31}P-\{^1H\}$ NMR spectra is highly correlated with proton resonances at δ4.17, δ3.65, and δ3.22, which can be readily assigned as PC. Peak β (δ_P 2.58) in the $^{31}P-\{^1H\}$ NMR spectra exhibited positive correlations with proton resonances at δ3.96 and δ3.24, which are consistent with the shifts for phosphorylethanolamine (PE). The most intense resonance in the $^{31}P-\{^1H\}$ spectra (δ_P 0.00) was uncorrelated with any ^1H NMR signals as it is from inorganic phosphate, which only has exchangeable protons, which do not give resolved signals in 1D NMR spectra. The level of correlation generated from the ^1H and $^{31}P-\{^1H\}$ NMR resonance intensities for PC and PE is shown in Figure 4, showing broadly linear correlations. By further examination of the HET-STOCSY (Figure 3), it was found that the PC peak intensity was correlated at a lower level with the intensity of resonances assigned to ascorbate (H4 at δ4.50 d, H5 at δ4.10 m) (Figure 5) and to glutathione (gln βCH_2 at δ2.20, gln δCH_2 at δ2.55, cys βCH_2 at δ2.95, gly αCH_2 at δ3.80, and cys αCH_2 at δ4.55) (Figure 3A). The assignment of ascorbate was confirmed by a two-dimensional $^1H-^1H$ TOCSY NMR spectrum as shown in Figure 5, indicating the expected cross-peaks. Such intermediate correlations are likely to be indicative of pathway-related correlations or metabolic coregulation.

Phospholipids are the major constituents of cell membranes, and oxidant-mediated injury to cells often involves cell membrane lipid peroxidation via free radicals. These processes are implicated in the development of several major pathologies, such as diabetes and cardiovascular disease.[37,38] Both ascorbate and glutathione are well-known antioxidants, and concurrence of both of the compounds in human gut tissues can be explained by the ascorbate−glutathione pathway.[39−41] The initial oxidation reaction utilizes ascorbate as an antioxidant and produces dehydroascorbate, and this process is catalyzed by ascorbate peroxidase. Ascorbate is then regenerated in a glutathione-dependent reaction catalyzed by dehydroascorbate reductase. Finally, the oxidized glutathione is reduced back to glutathione in a reaction involves glutathione reductase and NADPH. The regeneration of ascorbate is dependent on the availability of glutathione and hence modulated by the glutathione cycle. An antioxidant process via the ascorbate−glutathione pathway has subsequently been found widely in many plants.[39−41] Recently, the dependence of the recycling of ascorbate from its oxidized form on availability of NADPH was found in human endothelial cells.[42]

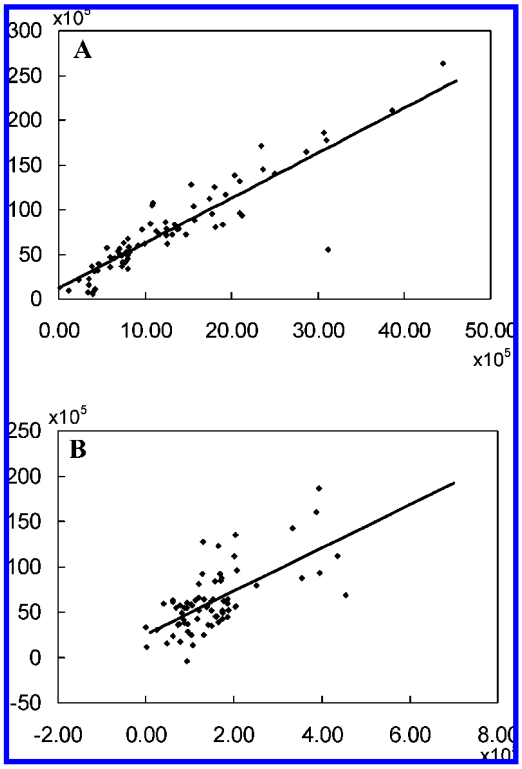

Figure 4. Graph showing the spectral intensity of ^1H and ^{31}P resonances for each spectrum, indicating the correlation between the $^{31}P-\{^1H\}$ and ^1H NMR peak intensities for (A) PC, $r^2 = 0.84$, and (B) PE, $r^2 = 0.43$.

The intensity of the $^{31}P-\{^1H\}$ NMR peak of PE had a positive covariance with ^1H NMR peaks from taurine (δ3.40 t, 3.24 t) (Figure 3B). A possible interrelationship between PE and taurine has been previously suggested by Lehmann and colleagues in the

(37) Mastorikou, M.; Mackness, M.; Mackness, B. *Diabetes* **2006**, *55*, 3099−3103.
(38) Tsimikas, S.; Kiechl, S.; Willeit, J.; Mayr, M.; Miller, E. R.; Kronenberg, F.; Xu, Q. B.; Bergmark, C.; Weger, S.; Oberhollenzer, F.; Witztum, J. L. *J. Am. Coll. Cardiol.* **2006**, *47*, 2219−2228.
(39) Dalton, D. A.; Russell, S. A.; Hanus, F. J.; Pascoe, G. A.; Evans, H. J. *Proc. Natl. Acad. Sci. U.S.A.* **1986**, *83*, 3811−3815.
(40) Nakano, Y.; Asada, K. *Plant Cell Physiol.* **1981**, *22*, 867−880.
(41) Foyer, C. H.; Halliwell, B. *Planta* **1977**, *133*, 21−25.
(42) May, J. M.; Qu, Z. C.; Neel, D. R.; Li, X. *Biochim. Biophys. Acta: Mol. Cell. Res.* **2003**, *1640*, 153−161.

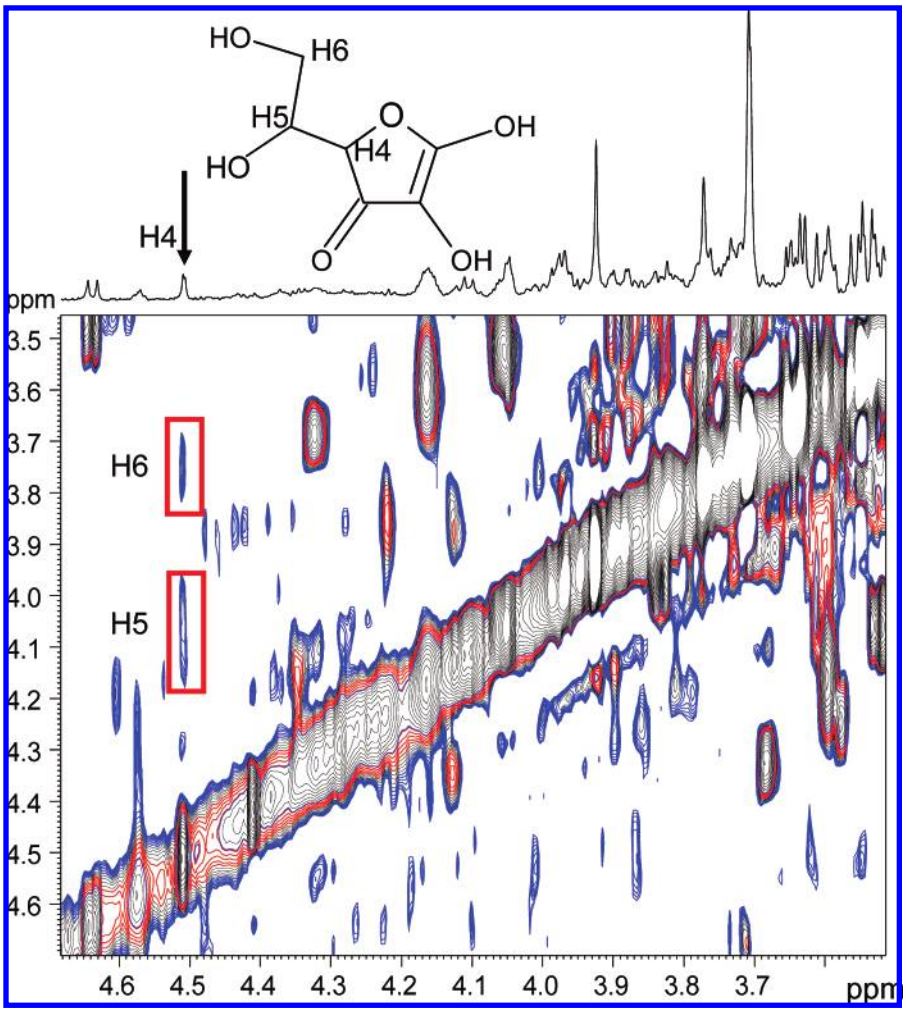

Figure 5. $^{1}H-^{1}H$ TOCSY MAS NMR spectrum of gut tissue showing the assignment of peaks corresponding to ascorbate. The CH peak of ascorbate at δ_H 4.47 is indicated by an arrow and the corresponding off-diagonal peaks showing the connectivity to the other protons of ascorbate are highlighted by the red boxes.

rat hippocampus (28−30). Evidence for this correlation comes from the fact that when taurine uptake was inhibited by guanidinoethanesulfonic acid, extracellular levels of both taurine and PE increased concurrently and when taurine was administered exogenously, the phosphorylethanolamine level also increased extracellularly.[43−45] The correlation between taurine and PE can be understood through the osmoprotective function of taurine. Taurine translocation through membranes is known *via* the Na^+- and Cl^--dependent amino acid transporter, TauT, and this process is activated by phospholipase-A2.[46] It is likely that PE is liberated from phosphatidylethanolamine by phospholipase enzymes, although further work needs to be carried out to verify the specific phospholipase to support this.

Cross-Correlation of $^{31}P-\{^{1}H\}$ and ^{1}H NMR Spectra for Information on Tissue Microenvironments. Another potential application of HET-STOCSY is to characterize relative differences in the composition of topographically dispersed tissues and to uncover information relating to compartmentalization of metabolites within such tissues. To exemplify the approach, the two-dimensional correlation matrix between the $^{31}P-\{^{1}H\}$ NMR spectra acquired from human gut biopsies from both combined jejunal and duodenal tissues and from tissue from transverse colon and the corresponding one-dimensional ^{1}H NMR spectra are shown in Figure 6A and B, respectively. These show the phosphodiester region of the $^{31}P-\{^{1}H\}$ NMR spectra and an expansion of part of the ^{1}H NMR spectra. Examination of individual $^{31}P-\{^{1}H\}$ NMR spectra showed that, when referenced to a constant chemical shift for phosphorylcholine, the phosphatidylcholine chemical shift is dependent on the tissue and thus the spectra contain a set of sharp peaks at variable chemical shifts that overlap to show the broad envelope between δ_P −0.5 and δ_P −2.5 seen in Figure 6. Small differences in tissue pH are to be expected, and this is shown by the variability in the ^{31}P NMR chemical shift of the inorganic phosphate as also seen in Figure 6. However, the observed chemical shift range for the phospholipids peaks is much greater, and since these are phosphodiesters with expected lower pH dependence, the wide spread in the observed shifts for the phospholipids probably arises from different environmental effects such as different types of compartmentation. In fact, to support this, dispersed ^{31}P NMR signals from lecithin have been observed

(43) Lehmann, A. *J. Neurochem.* **1989**, *53*, 525−535.
(44) Lehmann, A.; Lazarewicz, J. W.; Zeise, M. *J. Neurochem.* **1985**, *45*, 1172−1177.
(45) Lehmann, A.; Hamberger, A. *J. Neurochem.* **1984**, *42*, 1286−1290.
(46) Lambert, I. H. *Neurochem. Res.* **2004**, *29*, 27−63.

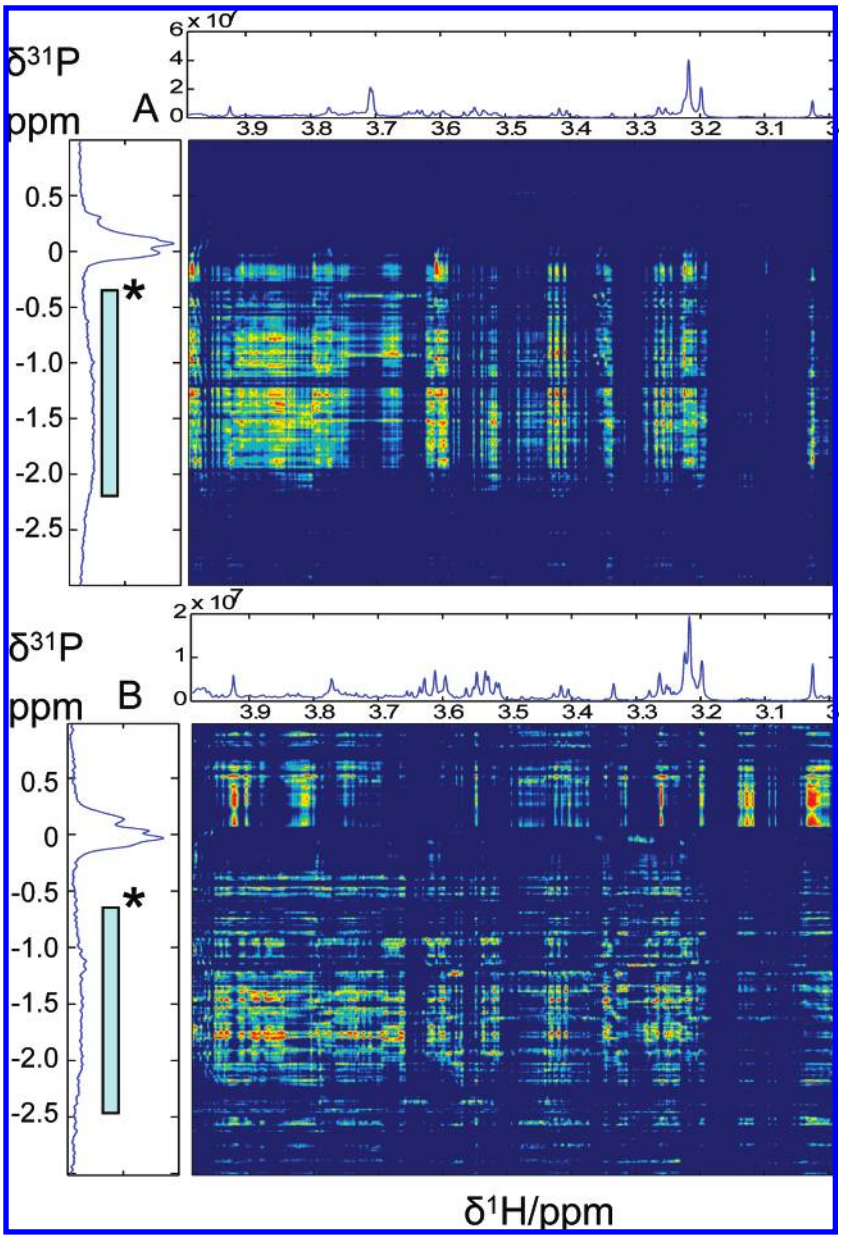

Figure 6. Two-dimensional HET-STOCSY correlation plots derived from $^{31}P-\{^{1}H\}$ and ^{1}H CPMG MAS NMR spectra of (A) jejunal and duodenal tissues (considered to be identical anatomically) and (B) transverse colon. indicating phospholipid profiles in different environments.

in vesicles formed with various concentrations of bile acids.[47] Thus, it may be assumed that the dispersion in the correlation matrix observed for phosphatidylcholine is not entirely a function of variation in pH, and other factors such as magnetic susceptibility differences are also likely to contribute to the ^{31}P shift variation. While all of the correlations between ^{31}P and ^{1}H chemical shifts in Figure 6A and B have not yet been identified, it is clear that, in both cases, all of the different ^{31}P NMR shifts from the different tissues that go to make up the broad envelope, correlate with the same peaks in the ^{1}H NMR spectra, indicating that the ^{31}P peaks all come from phosphatidylcholine present in a range of compartments/environments. This is supported by the fact that strong correlations are seen to the $N^{+}Me_3$ peak at δ3.22 and the NCH_2 peak at δ3.65. It is noted that the phosphatidylcholine chemical shift range observed in the ^{31}P NMR spectra is not evident in the ^{1}H NMR spectra, consistent with the greater sensitivity of ^{31}P NMR shifts to variations in the physicochemical properties of the solutions.

Other correlations are likely to be to the ^{1}H NMR signals of metabolites in the same biochemical pathway as phosphatidylcholine, i.e., its precursors and degradation products and a detailed analysis of these correlations is ongoing.

Strong correlations are observed between ^{1}H and ^{31}P signals at δ_{31P} 0.0−0.5 (Figure 6B), although there is little signal intensity in the 1D ^{31}P NMR spectra. This could be an example of the correlation behavior of STOCSY plot resulting in a net signal integration of chemical noise (multiple overlapped low level signals in the 1D spectra[33,48]). However, while these peaks remain as yet

(47) Ben, Mouaz, A.; Lindheimer, M.; Montet, J. C.; Zajac, J.; Lagerge, S. *Colloids Surf.. B: Biointerfaces* **2001**, *20*, 119−127.

(48) Wilson, I. D.; Fromson, J.; Ismail, I. M.; Nicholson, J. K. *J. Pharm. Biomed. Anal.* **1987**, *5*, 157−163.

unidentified, strong correlations are seen to the creatine peaks in the ^{1}H NMR spectra, implying the probable involvement of the phosphocreatine/creatine kinase pathway. Overall by suitable correlation and variation of pH and temperature, together with NMR parameters such as field gradient strength in diffusion-edited spectra (for ^{1}H and ^{31}P) or spin−echo delays, it should be possible to explore multilevel compartmentation in soft tissues as examined by MAS NMR spectroscopy.

CONCLUSIONS

Application of STOCSY to homonuclear NMR spectra has been proven to be successful in the identification of NMR resonance of both endogenous and xenobiotic molecules based on highly correlated peak intensities.[36] The same technique has now been applied to the ^{1}H NMR spectra obtained from different homonuclear pulse sequences or from a series of NMR spectra obtained from different nuclei. It was possible to unambiguously assign ^{31}P NMR signals to specific molecules from a series of one-dimensional ^{1}H NMR spectra, and this overcomes the disadvantage of the insensitivity of many heteronuclear NMR-active nuclei or the lack of ^{1}H-heteronucleus spin interactions. In addition, detection of molecules in the same metabolic pathway was achieved based on the covariance of spectral intensities from these metabolites, hence providing insight into biological pathways in these tissues. Furthermore, this technique was also able to recover tissue microcompartmental metabolic information present in the system, such as the detection of triglycerides in lipid vesicles within cells in intact tissue.

The principle of HET-STOCSY is widely applicable to other biological or chemical systems where any two different homo- or heteronuclear NMR spectra are measured on a series of samples. This approach has the advantage that *J*-coupling and NOE interactions are not required, but only that the samples contain a range of concentrations of the same molecules. Moreover, application of HET-STOCSY to multiple sample MR spectra acquired in vivo should be possible to enhance the sensitivity of the measurement and to identify metabolites in spectra where *J*-coupling is usually not observed.

ACKNOWLEDGMENT

The clinical trial was performed at the *centre hospitalier universitaire vaudóis (CHUV), Lausanne,* Switzerland, and we thank both the staff of that centre and the participants who took part in the study. This work was funded by Nestec S.A., Switzerland. H.T. acknowledges China NSFC (20575074), the Chinese Academy of Sciences (100T program 2005[35]-T12508-O6S138), and National Basic Research Program of China (2006CB503909) for financial supports.

Received for review September 21, 2007. Accepted November 27, 2007.

AC701988A